Applied Physics Letters ARTICLE scitation.org/journal/apl

Energy levels and charge state control of the carbon antisite-vacancy defect in 4H-SiC

Cite as: Appl. Phys. Lett. **114**, 212105 (2019); doi: 10.1063/1.5098070
Submitted: 31 March 2019 · Accepted: 16 May 2019 ·
Published Online: 31 May 2019

Nguyen Tien Son,[1,a)] Pontus Stenberg,[1,b)] Valdas Jokubavicius,[1] Hiroshi Abe,[2] Takeshi Ohshima,[2] Jawad Ul Hassan,[1] and Ivan G. Ivanov[1]

AFFILIATIONS

[1]Department of Physics, Chemistry and Biology, Linköping University, SE-58183 Linköping, Sweden
[2]National Institutes for Quantum and Radiological Science and Technology, 1233 Watanuki, Takasaki, Gunma 370-1292, Japan

[a)]tien.son.nguyen@liu.se
[b)]**Present address:** Ascatron AB, Electrum 207, SE-16440 Kista, Sweden.

ABSTRACT

The carbon antisite-vacancy pair ($C_{Si}V_C$) in silicon carbide (SiC) has recently emerged as a promising defect for applications in quantum communication. In the positive charge state, $C_{Si}V_C^+$ can be engineered to produce ultrabright single photon sources in the red spectral region, while in the neutral charge state, it has been predicted to emit light at telecom wavelengths and to have spin properties suitable for a quantum bit. In this electron paramagnetic resonance study using ultrapure compensated isotope-enriched 4H-^{28}SiC, we determine the (+|0) level of $C_{Si}V_C$ and show that the positive and neutral charge states of the defect can be optically controlled.

Defect spins in silicon carbide (SiC) have recently shown to be promising for applications in quantum communication[1–13] and sensing.[14–19] Among these, the Si vacancy (V_{Si}), divacancy ($V_{Si}V_C$), and C antisite-vacancy pair ($C_{Si}V_C$) have attracted great attention due to their favorable optical and spin properties and the well-controlled fabrication of single photon sources.[5–7] While single spins associated with the negative Si vacancy (V_{Si}^-) and the neutral divacancy ($V_{Si}V_C^0$) are shown to have long coherence time and can be optically initialized, controlled, and read out with high fidelity,[6,7,12,13] the positive $C_{Si}V_C^+$ pair can be engineered to ultrabright single photon sources.[5] Interestingly, a recent calculation[20] predicts that the neutral $C_{Si}V_C^0$ defect is a photoluminescence (PL) center emitting light at telecom wavelengths and can be a promising solid-state quantum bit for integration of quantum optics devices with existing fiber optics technology. So far, the reported single photon emitters, based on trapped ions in a lattice, quantum dots, or color centers in condensed matters, emit lights in visible or near-infrared spectral regions. Their application in this field requires quantum down frequency conversion to convert their emissions into telecom wavelength bands. This process generates noises and causes intensity loss. Therefore, $C_{Si}V_C^0$ can be a very important color center for quantum communication.

The $C_{Si}V_C$ pair is a fundamental defect in SiC. It is a counterpart of the Si vacancy[21] and can be created by high-energy-particle radiation and subsequent annealing at ∼700–750 °C (Ref. 22) when a V_{Si} traps a nearest C neighbor. One of the four configurations of this defect in the single negative charge state has been identified by electron paramagnetic resonance (EPR) in n-type 4H-SiC.[22] Density functional calculations (DFT) predict the (0|−) level of $C_{Si}V_C$ to be at ∼1.0 eV below the conduction band (CB), i.e., $\sim E_C - 1.0$ eV.[22] The positively charged state of the $C_{Si}V_C$ defect has also been identified in 4H-SiC.[23] EPR studies of irradiated p-type materials suggested that the electronic level of $C_{Si}V_C^+$ is located at ∼1.4–1.5 eV above the valence band (VB), i.e., $\sim E_V + (1.4–1.5)$ eV.[23] It is also shown from previous studies that the neutral charge state of the defect, $C_{Si}V_C^0$, is not accessible in n-type[22] and p-type[23] materials.

A recent hybrid functional calculation[20] predicted energy levels for different charge states of $C_{Si}V_C$ in 4H-SiC: $\sim E_C - (0.5–0.6)$ eV, $\sim E_C - (1.1–1.15)$ eV, and $\sim E_V + (1.28–1.36)$ eV, for the (0|−), (+|0), and (++|+) levels, respectively. However, the single donor and neutral states of $C_{Si}V_C$ are significantly higher in the bandgap compared to the corresponding levels reported in previous studies.[23] With the single donor level (+|0) lying higher in the bandgap compared to other known common intrinsic defects, such as the C vacancy (V_C) (at $\sim E_C - 1.55$ eV, Ref. 24) and V_CV_{Si} (at $\sim E_V + 1.1$ eV, Ref. 25), the $C_{Si}V_C$ center is anticipated to play an important role in carrier compensation in compensated or p-type materials. So far, these calculated levels of $C_{Si}V_C$ have not been experimentally confirmed.

In this letter, we present our EPR studies of the $C_{Si}V_C$ defect in ultrapure isotope-enriched 4H-^{28}SiC. With the ^{28}Si isotope (nuclear

spin I = 0) enriched to 99.85%, the hyperfine (hf) structures due to the interaction between the electron spin and the nuclear spins of ^{29}Si atoms (I = 1/2) are absent for all defects and the linewidth of EPR signals becomes very narrow. We are, therefore, able to observe clear signals from all four possible configurations of the $C_{Si}V_C$ center and accurately determine the line intensity in photo-excitation EPR (photo-EPR). From the optical transitions that activate and deactivate the $C_{Si}V_C^+$ signal, the (+|0) level of this defect is determined to be at ∼1.1 eV below the CB. In addition, we show that the positive and neutral charge states of $C_{Si}V_C$ can be effectively controlled by optical excitation.

The starting material used in this study is an isotopically purified 4H-^{28}SiC epilayer grown by chemical vapor deposition (CVD).[26] The isotope purity of ^{28}Si in this layer is expected to be 99.85%, which is the value determined by secondary ion mass spectrometry (SIMS) for other isotopically enriched 4H-^{28}Si^{12}C wafers grown in the series.[27] Free-standing 4H-^{28}SiC CVD layers with a thickness of ∼250 μm are obtained after removing the substrate by mechanical polishing. After polishing, the layers are annealed at 1130 °C to reduce the concentration of paramagnetic defects at the surface created by polishing. Annealing is performed in N_2 gas flow to avoid oxidation. The residual N concentration of the layer is $\sim 5 \times 10^{12}$ cm^{-3} as estimated from PL.[28] Another common unintentionally incorporated impurity is B, which comes from the susceptor with a typical concentration of 1×10^{13} cm^{-3}. Deep level transient spectroscopy measurements of the $Z_{1/2}$ and $EH_{6/7}$ centers, which are known to be related to the double acceptor and single donor levels, respectively, of the C vacancy,[24] show a typical concentration of V_C in the low to mid 10^{13} cm^{-3} range.[29]

The samples are irradiated by 2-MeV electrons at room temperature to a dose of 4×10^{18} cm^{-2} and annealed at 820 °C to remove interstitial-related defects and to form $C_{Si}V_C$. EPR measurements are performed on an X-band (∼9.4 GHz) Bruker E500 EPR spectrometer equipped with a He-flow cryostat, allowing sample temperature regulation in the range of 4–300 K. For optical excitation, a 200 W halogen lamp, which provides a broad radiation band ranging from ∼350 nm to ∼4000 nm with the maximum power at ∼900 nm, and a 0.25 m single grating Jobin-Yvon monochromator are used as a light source. The studied wavelength range of 500–1600 nm in our experiments corresponds to the strong part of radiation spectral of the lamp (radiation power at 500 nm and 1600 nm is about 40% and 60% of its maximum, respectively, when operating at 180 W power). In photo-EPR experiments, we use a 600 g/mm grating which gives a dispersion of 3.2 nm/mm. With a fully open slit (3 mm), the bandwidth of the excitation is 9.6 nm.

In the as-grown layer, the N shallow donor is completely compensated by the B acceptor. Uncompensated B acceptors are then compensated by V_C. As a result, the layer becomes highly resistive, resulting in a high value of the Q-factor of the EPR cavity at a room temperature of about 9000. Measurements on the as-grown layers after annealing at 1130 °C do not show any EPR signal, neither at 10 K nor at room temperature, indicating that the concentration of the surface defects is below the detection limit and the shallow N donor and B acceptor are completely compensated.

The EPR spectrum of the as-irradiated sample observed in darkness at room temperature is dominated by the negative Si vacancy (V_{Si}^-) and other interstitial-related defects. The sample is annealed at 820 °C to remove interstitial-related defects and to form $C_{Si}V_C$. The EPR spectrum measured in darkness at room temperature for the magnetic field along the c-axis (**B**||**c**) shows the dominating signal of the V_{Si}^- center (Fig. 1). The lines labeled T_{V1a} and T_{V2a} in the figure correspond to two configurations of V_{Si}^- at the hexagonal (*h*) and quasicubic (*k*) lattice sites of 4H-SiC, respectively.[30] The hf structures due to the interaction between the electron spin and the nuclear spin of a ^{13}C (I = 1/2, natural abundance 1.1%) occupying one of the four nearest C neighbors of V_C can be seen in the spectrum plotted with the intensity-extended scale.

In addition to the V_{Si}^- signal, a sharp and weaker line, marked as $C_{Si}V_C^+$ in Fig. 1, is observed. This line shows a weak pair of hf lines with a splitting of 82.5 G (see the intensity-extended scale spectrum in Fig. 1). This line belongs to a C_{3v} center with g-values of $g_{||} = 2.00243$ and $g_\perp = 2.00403$. The intensity ratio between the two hf lines and the main line is ∼1%, indicating that these hf lines are from the interaction with one ^{13}C. The C hf parameters are determined as $A_{||} = 82.5$ G and $A_\perp = 23.0$ G. Comparing these g-values and C hf parameters with the corresponding values of the $C_{Si}V_C^+$ center reported previously, we can identify that this line belongs to $C_{Si}V_C^+$ at the *hh* site in 4H-SiC ($g_{||} = 2.00227$ and $g_\perp = 2.00408$; $A_{||} = 82.5$ G and $A_\perp = 22.7$ G, Ref. 23).

Figure 2 shows the EPR spectrum measured for **B**||**c** using a lower microwave (MW) power of 6.325 μW and a very low field modulation of 0.01 G. Under such measuring conditions, the linewidth of $C_{Si}V_C^+$ reduces to ∼0.08 G (as counting from the maximum to minimum of the absorption line) and two lines corresponding to the *hh* and *kh* configurations of this center could be well resolved. It is noticed further that in darkness at room temperature, we observe only two configurations *hh* and *kh* of $C_{Si}V_C^+$, while in the previous study by Umeda and co-workers,[23] all four configurations are detected. This is most likely due to the difference in the starting materials. In the B-doped p-type substrate, the compensation of a high concentration of B acceptors leads to the activation of both $C_{Si}V_C^+$ and V_C^+ centers as detected by EPR in darkness.[23] In our material, the B concentration is only $\sim 1 \times 10^{13}$ cm^{-3}. The acceptor levels lying below the single donor

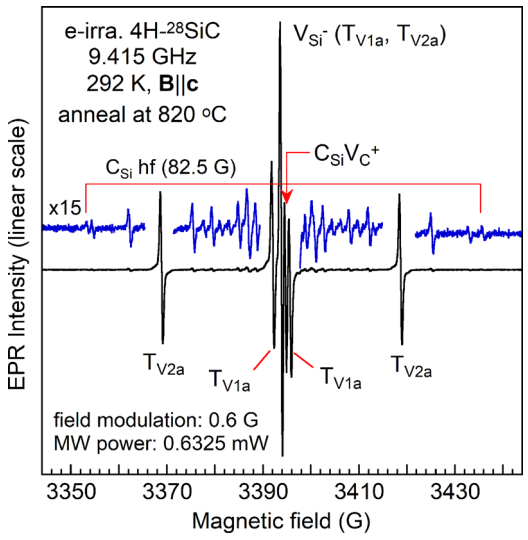

FIG. 1. EPR spectrum in irradiated and annealed 4H-^{28}SiC measured at 292 K for **B**||**c** showing the signals of the V_{Si}^- centers T_{V1a} and T_{V2a} and the $C_{Si}V_C^+$ center in the axial *hh* configuration. The hf lines of the C antisite, C_{Si}, are indicated in the spectrum with the intensity-extended scale.

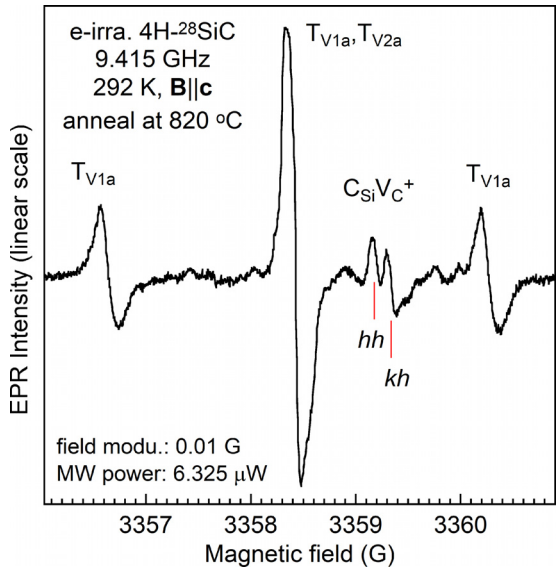

FIG. 2. The EPR spectrum in Fig. 1 measured with a very low field modulation of 0.01 G and a lower MW power of 6.325 μW showing resolved lines corresponding to the *hh* and *kh* configurations of the $C_{Si}V_C^+$ center. Here, we follow the assignment of these defect configurations in Ref. 23.

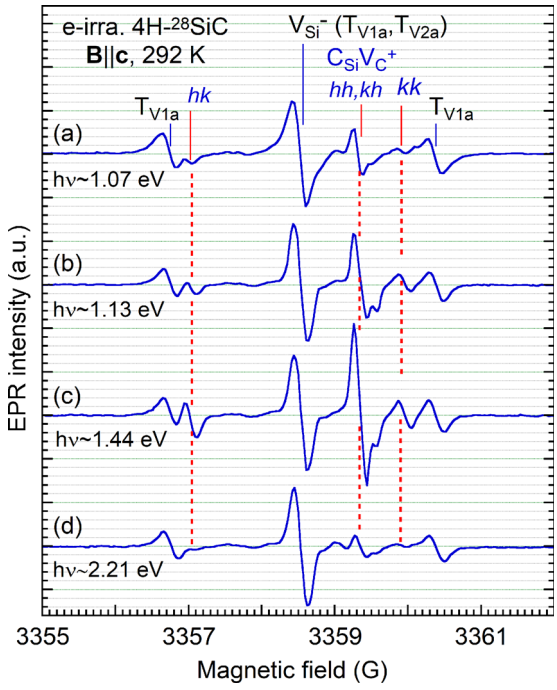

FIG. 3. EPR spectra in irradiated and annealed 4H-^{28}SiC measured at 292 K for **B||c** under illumination with light of different photon energies: (a) ~1.07 eV, (b) ~1.13 eV, (c) ~1.44 eV, and (d) ~2.21 eV. All the spectra are measured with a field modulation of 0.2 G and a MW power of 0.6325 mW. The lines corresponding to different configurations of $C_{Si}V_C^+$ are indicated. For all spectra, the MW frequency is calibrated to be 9.415 GHz. The spectra are plotted with the shifted zero level on the same intensity scale and can be directly compared with each other. It is noticed that although the V_{Si}^- signal has a higher intensity than $C_{Si}V_C^+$, its concentration is lower since the spin is 3/2 for V_{Si}^- and 1/2 for $C_{Si}V_C^+$.

level (+|0) of $C_{Si}V_C$ are V_{Si}^- (at ~E_V + 1.25 eV, Ref. 20) and $V_CV_{Si}^-$ (at ~E_C − 1.3 eV, Ref. 25). After annealing at 820 °C, the concentration of V_{Si}^- is ~1×10^{15} cm^{-3} as estimated by EPR. Under strong optical excitation (without a monochromator), the concentrations of $V_CV_{Si}^0$ and V_C^- are estimated to be ~8×10^{15} cm^{-3} and low 10^{16} cm^{-3}, respectively. It seems that the concentration of $C_{Si}V_C$ is higher than that of the Si vacancy and divacancy so that the electron trapping process to change the charge state of V_{Si} and V_CV_{Si} from neutral to negative leads to the ionization of only two configurations *hh* and *kh* of $C_{Si}V_C$ with higher-lying energy levels, while other two configurations *kk* and *hk* remain in the neutral charge state and are not detected (Fig. 2). This explains our observation of only the $C_{Si}V_C^+(hh)$ and $C_{Si}V_C^+(kh)$ signals in darkness. Thus, in our sample, the Fermi level is located at the (+|0) level of $C_{Si}V_C(hh)$ and $C_{Si}V_C(kh)$ configurations, keeping the V_C and $V_{Si}V_C$ centers in the neutral and single negative charge states, respectively. Therefore, the V_C^+ and $V_{Si}V_C^0$ signals are not detected in darkness.

We have also checked EPR at low temperatures and in a wider magnetic field range to look for the signal of the neutral $C_{Si}V_C^0$ center, which is predicted to have a spin S = 1 ground state and C_{1h} symmetry.[20] Several S = 1 EPR centers with C_{3v} and C_{1h} symmetry are detected. However, in this isotope-enriched 4H-^{28}SiC, Si hf structures vanish, which makes the defect identification difficult. The identification of the neutral charge state of $C_{Si}V_C$ is beyond the scope of this letter and will not be discussed further.

Figure 3 shows EPR spectra measured at 292 K for **B||c** under illumination by light of different photon energies. In the figure, all the spectra are plotted with the shifted zero level on the same intensity scale and can be directly compared with each other. As noticed earlier (cf. Fig. 2), only two configurations *hh* and *kh* of $C_{Si}V_C^+$ appear in the spectrum measured in darkness. For increasing the signal intensity, we use a higher MW power of 0.6325 mW in the photo-EPR experiments. When the photon energy reaches $h\nu \sim 1.07$ eV, two lines from the other two configurations not seen in dark, *kk* and *hk*, weakly emerge from the noise level [Fig. 3(a)] and become distinct when $h\nu \sim 1.13$ eV [Fig. 3(b)]. All the lines from four configurations exhibit a rapid increase in intensity when the photon energy exceeds ~1.07 eV. The $C_{Si}V_C^+$ signal becomes even stronger than the V_{Si}^- signal for the photon energy in the range of 1.17–1.63 eV [Fig. 3(c)]. With a further increase in the photon energy, the $C_{Si}V_C^+$ signal decreases. For $h\nu \sim 2.2$ eV, the signals of the *kk* and *hk* configurations approach the noise level while the line corresponding to the *hh* and *kh* configurations becomes even weaker than it is measured in darkness [Fig. 3(d)].

The concentration of $C_{Si}V_C^+$ estimated from the strongest EPR line of the *hh* and *kh* configurations activated by weak optical excitation in Fig. 3(c) is ~7×10^{15} cm^{-3}. Thus, the total concentration of four configurations of the $C_{Si}V_C$ defect is expected to be in the low 10^{16} cm^{-3} range or higher since only a part of its total concentration is activated in the positive charge state. The V_{Si}^- signal does not show a noticeable change under photoexcitation.

The integrated intensities of these four configurations of the $C_{Si}V_C^+$ center vs the photon energy are shown in Fig. 4. With the MW power of 0.6325 mW, the signals of $C_{Si}V_C^+(hh)$ and $C_{Si}V_C^+(kh)$ are not resolved and, therefore, the intensity estimated for this line

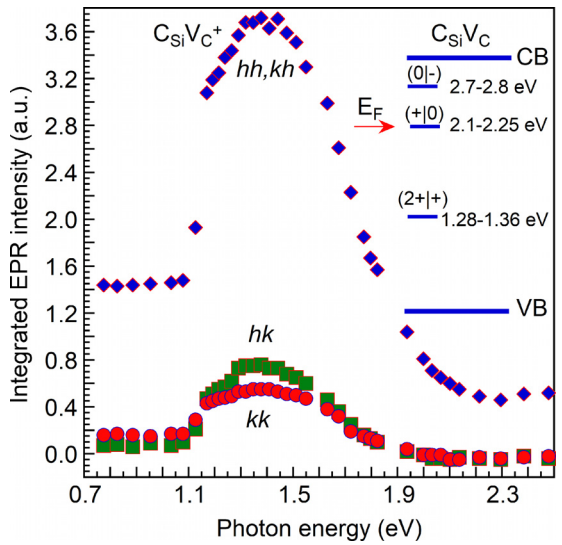

FIG. 4. The dependence of the integrated EPR intensity of different configurations of the $C_{Si}V_C^+$ center on the photon energies. The inset shows the energy levels of different charge states of $C_{Si}V_C$ obtained from hybrid functional calculations.[20]

represents the joint contribution of these two configurations. Within the experimental errors, all configurations of $C_{Si}V_C$ show a similar energy threshold of ~1.1 eV for the activation of the positive charge state. This observation can be explained by the energy diagram for $C_{Si}V_C$ obtained from calculations[20] given in the inset of Fig. 4. Photons with energies ≥1.1 eV can excite electrons from the (+|0) level to the CB, thus transforming $C_{Si}V_C^0$ to $C_{Si}V_C^+$, which is detected by EPR.

We now discuss a possible explanation of the saturation and decrease in the signals from all $C_{Si}V_C^+$ configurations for photon energies $h\nu > \sim 1.3$ eV. When the photon energy exceeds ~1.3 eV, light can also excite electrons from the (−|0) and (−|2−) levels of the divacancy (at ~1.3 eV and ~1.2 eV below the CB, respectively).[25] As a result, the concentration of free electrons in the CB drastically increases. The rate of electron removal from the divacancy will increase with increasing photon energy since the density of states in the CB grows with the square root of the energy above the CB edge. Furthermore, owing to the long-range Coulomb interaction, the capture of free electrons to the positively charged $C_{Si}V_C^+$ is much faster than electron capture to the neutral or singly negatively charged divacancies. This accelerates the process of electron capture to $C_{Si}V_C^+$, leading to the conversion of the charge state of the defect to neutral. Thus, the competition between the two processes, the electron removal from and capture to $C_{Si}V_C$, can be seen as the reason leading to saturation and a decrease in the $C_{Si}V_C^+$ signal for photon energies $h\nu > \sim 1.3$ eV as shown in Fig. 4.

When the photon energy reaches ~2.1 eV, light can also excite electrons from the VB to the (+|0) level of $C_{Si}V_C$ at the *kk* and *hk* configurations and change their charge state from positive to neutral, leading to the disappearance of the $C_{Si}V_C^+(kk)$ and $C_{Si}V_C^+(hk)$ signals (Fig. 4). A similar process occurs for the $C_{Si}V_C^+(hh)$ and $C_{Si}V_C^+(kh)$ centers when $h\nu \geq 2.3$ eV since the (+|0) level of these two configurations lies slightly higher in the bandgap. Thus, in such pure and compensated materials, the neutral charge state of $C_{Si}V_C$ can be efficiently activated by light of photon energies larger than ~2.3 eV. Both the optical transitions to the CB and from the VB of the (+|0) level of $C_{Si}V_C$ are also in good agreement with the predicted level from calculations.[20]

As shown in a previous study, in irradiated n-type materials, $C_{Si}V_C$ is mainly in the double negative (2−) charge state and illumination can activate the single negative charge state but not the neutral charge state of this defect.[22] In irradiated p-type 4H-SiC, the EPR signals of both $C_{Si}V_C^+$ and V_C^+ centers are already detected in darkness.[23] Since the Fermi-level window for $C_{Si}V_C^+$ is very large, stretching between the (++|+) level at ~E_V + 1.3 eV and the (+|0) level at ~E_V + (2.1–2.2) eV,[20] the observation of both the $C_{Si}V_C^+$ and V_C^+ signals in p-type 4H-SiC[23] indicates that the Fermi level should be located at the (+|0) level of V_C. In this situation, pumping electrons from the VB to the (++|+) level to change the charge state of $C_{Si}V_C$ from positive to neutral requires light with photon energies of $h\nu \geq 1.3$ eV. However, this photon energy can also efficiently remove electrons from the (+|0) level at ~ E_C − 1.1 eV to the CB and, therefore, it is difficult to activate the neutral charge state of $C_{Si}V_C$. This explains why illumination does not show a clear effect on the EPR signal of $C_{Si}V_C^+$ in irradiated p-type 4H-SiC.[23]

In summary, using ultrapure compensated isotope-enriched 4H-^{28}SiC, we could clearly observe all four configurations of the $C_{Si}V_C^+$ center in EPR and their response to illumination in photo-EPR experiments. Our photo-EPR results suggest that the (+|0) energy level of $C_{Si}V_C$ is located at ~1.1 eV below the CB which is in very good agreement with theoretical calculations. Our photo-EPR also shows that using pure compensated materials, both the positive and neutral charge states of the $C_{Si}V_C$ center can be effectively controlled by optical excitation. The neutral charge state of $C_{Si}V_C$ may also be accessible even in the p-type material if the concentration of this defect is still larger than the total concentration of shallow acceptors and the divacancy so that only a part of it is being positively charged.

Support from the Swedish Research Council (Nos. VR 2016-04068 and VR 2016-05362), the Swedish Energy Agency (No. 43611-1), the Knut and Alice Wallenberg Foundation (No. KAW 2018.0071), and the Japan Society for Promotion of Science KAKENHI (Nos. 17H01056 and 18H03770) is acknowledged.

REFERENCES

[1]W. F. Koehl, B. B. Buckley, F. J. Heremans, G. Calusine, and D. D. Awschalom, Nature **479**, 84 (2011).
[2]P. G. Baranov, A. P. Bundakova, A. A. Soltamova, S. B. Orlinskii, I. V. Borovykh, R. Zondervan, R. Verberk, and J. Schmidt, Phys. Rev. B **83**, 125203 (2011).
[3]D. Riedel, F. Fuchs, H. Kraus, S. Väth, A. Sperlich, V. Dyakonov, A. A. Soltamova, P. G. Baranov, V. A. Ilyin, and G. V. Astakhov, Phys. Rev. Lett. **109**, 226402 (2012).
[4]V. A. Soltamov, A. A. Soltamova, P. G. Baranov, and I. I. Proskuryakov, Phys. Rev. Lett. **108**, 226402 (2012).
[5]S. Castelletto, B. C. Johnson, V. Ivády, N. Stavrias, T. Umeda, A. Gali, and T. Ohshima, Nat. Mater. **13**, 151 (2014).
[6]M. Widmann, S.-Y. Lee, T. Rendler, N. T. Son, H. Fedder, S. Paik, L.-P. Yang, N. Zhao, S. Yang, I. Booker, A. Denisenko, M. Jamali, S. A. Momenzadeh, I. Gerhardt, T. Ohshima, A. Gali, E. Janzén, and J. Wrachtrup, Nat. Mater. **14**, 164 (2015).
[7]D. J. Christle, A. L. Falk, P. Andrich, P. V. Klimov, J. U. Hassan, N. T. Son, E. Janzén, T. Ohshima, and D. D. Awschalom, Nat. Mater. **14**, 160 (2015).
[8]F. Fuchs, B. Stender, M. Trupke, D. Simin, J. Pflaum, V. Dyakonov, and G. V. Astakhov, Nat. Commun. **6**, 7578 (2015).

[9]H. J. von Bardeleben, J. L. Cantin, E. Rauls, and U. Gerstmann, Phys. Rev. B **92**, 064104 (2015).
[10]A. Lohrmann, N. Iwamoto, Z. Bodrog, S. Castelletto, T. Ohshima, T. J. Karle, A. Gali, S. Prawer, J. C. McCallum, and B. C. Johnson, Nat. Commun. **6**, 7783 (2015).
[11]M. Radulaski, M. Widmann, M. Niethammer, J. L. Zhang, S.-Y. Lee, T. Rendler, K. G. Lagoudakis, N. T. Son, E. Janzen, T. Ohshima, J. Wrachtrup, and J. Vučković, Nano Lett. **17**, 1782 (2017).
[12]D. J. Christle, P. V. Klimov, C. F. de las Casas, K. Szász, V. Ivády, V. Jokubavicius, J. Ul Hassan, M. Syväjärvi, W. F. Koehl, T. Ohshima, N. T. Son, E. Janzén, A. Gali, and D. D. Awschalom, Phys. Rev. X **7**, 021046 (2017).
[13]R. Nagy, M. Niethammer, M. Widmann, Y.-C. Chen, P. Udvarhelyi, C. Bonato, J. Ul Hassan, R. Karhu, I. G. Ivanov, N. T. Son, J. R. Maze, T. Ohshima, Ö. O. Soykal, A. Gali, S.-Y. Lee, F. Kaiser, and J. Wrachtrup, Nat. Commun. **10**, 1954 (2019).
[14]H. Kraus, V. A. Soltamov, F. Fuchs, D. Simin, A. Sperlich, P. G. Baranov, G. V. Astakhov, and V. Dyakonov, Sci. Rep. **4**, 5303 (2014).
[15]D. Simin, F. Fuchs, H. Kraus, A. Sperlich, P. G. Baranov, G. V. Astakhov, and V. Dyakonov, Phys. Rev. Appl. **4**, 014009 (2015).
[16]D. Simin, V. A. Soltamov, A. V. Poshakinskiy, A. N. Anisimov, R. A. Babunts, D. O. Tolmachev, E. N. Mokhov, M. Trupke, S. A. Tarasenko, A. Sperlich, P. G. Baranov, V. Dyakonov, and G. V. Astakhov, Phys. Rev. X **6**, 031014 (2016).
[17]M. Niethammer, M. Widmann, S.-Y. Lee, P. Stenberg, O. Kordina, T. Ohshima, N. T. Son, E. Janzén, and J. Wrachtrup, Phys. Rev. Appl. **6**, 034001 (2016).
[18]C. J. Cochrane, J. Blacksberg, M. A. Anders, and P. M. Lenahan, Sci. Rep. **6**, 37077 (2016).
[19]G. Wolfowicza, S. J. Whiteleya, and D. D. Awschalom, Proc. Natl. Acad. Sci. **115**, 7879 (2018).
[20]K. Szász, V. Ivády, I. A. Abrikosov, E. Janzén, M. Bockstedte, and A. Gali, Phys. Rev. B **91**, 121201(R) (2015).
[21]E. Rauls, T. Lingner, Z. Hajnal, S. Greulich-Weber, T. Frauenheim, and J.-M. Spaeth, Phys. Status Solidi B **217**, r1 (2000).
[22]T. Umeda, N. T. Son, J. Isoya, E. Janzén, T. Ohshima, N. Morishita, H. Itoh, A. Gali, and M. Bockstedte, Phys. Rev. Lett. **96**, 145501 (2006).
[23]T. Umeda, J. Isoya, T. Ohshima, N. Morishita, H. Itoh, and A. Gali, Phys. Rev. B **75**, 245202 (2007).
[24]N. T. Son, X. T. Trinh, L. S. Løvlie, B. G. Svensson, K. Kawahara, J. Suda, T. Kimoto, T. Umeda, J. Isoya, T. Makino, T. Ohshima, and E. Janzén, Phys. Rev. Lett. **109**, 187603 (2012).
[25]B. Magnusson, N. T. Son, A. Csóré, A. Gällström, T. Ohshima, A. Gali, and I. G. Ivanov, Phys. Rev. B **98**, 195202 (2018).
[26]P. Stenberg, P. Sukkaew, I. Farkas, O. Kordina, E. Janzén, L. Ojamäe, Ö. Danielsson, and H. Pedersen, J. Phys. Chem. C **121**, 2711 (2017).
[27]I. G. Ivanov, M. Yazdanfar, B. Lundqvist, J.-T. Chen, J. Hassan, P. Stenberg, R. Liljedahl, N. T. Son, J. W. Ager III, O. Kordina, and E. Janzén, Mater. Sci. Forum **778–780**, 471 (2014).
[28]I. G. Ivanov, C. Hallin, A. Henry, O. Kordina, and E. Janzén, J. Appl. Phys. **80**, 3504 (1996).
[29]P. Stenberg, I. D. Booker, R. Karhu, H. Pedersen, E. Janzén, and I. G. Ivanov, Physica B **535**, 44 (2018).
[30]N. T. Son, P. Stenberg, V. Jokubavicius, T. Ohshima, J. Ul Hassan, and I. G. Ivanov, J. Phys.: Condens. Matter **31**, 195501 (2019).